Original Article

Enhanced Cognitive and Behavioral Function as well as Neurobiochemical Enzyme Activities in Aluminum-Exposed Rats through Cerium Oxide Nanoparticles (CeO2 NPs)

Davoud Malekzadeh[1], Arash Abdolmaleki[2*], Gholamreza Dehghan[1*], Asadollah Asadi, Amirreza ghabaei[3], Hussein A.Ghanimi[4,5]

1. *Department of Biology, Faculty of Natural Science, University of Tabriz, Tabriz, Iran.*
2. *Department of Biophysics, Faculty of Advanced Technologies, University of Mohaghegh Ardabili, Namin, Iran.*
3. *Department of Biology, Faculty of Science, University of Mohaghegh Ardabili, Ardabil, Iran.*
4. *College of Nursing, University of Al-Ameed, Karbala, Iraq*
5. *Department of Clinical Laboratories, College of Applied Medical Sciences, University of Kerbala, Karbala, Iraq.*

How to cite this article: **Davoud Malekzadeh, Arash Abdolmaleki, Gholamreza Dehghan, Asadollah Asadi, Amirreza ghabaei, Hussein A.Ghanimi. Enhanced Cognitive and Behavioral Function as well as Neurobiochemical Enzyme Activities in Aluminum-Exposed Rats through Cerium Oxide Nanoparticles (CeO2 NPs). Archives of Razi Institute. 2025;80(2):537-549.**
DOI: 10.32592/ARI.2025.80.2.537

Article Info:
Received: 13 April 2024
Accepted: 9 June 2024
Published: 30 April 2025

Corresponding Author's E-Mail:
Abdolmalekiarash1364@gmail.com
dehghan2001d@yahoo.com

ABSTRACT

Neurological and behavioral diseases caused by toxic metals, particularly aluminum, continue to pose a substantial issue for humans. Given the prevalence of aluminum in the Earth's crust, it is inevitable that humans worldwide will have contact with aluminum. The present study focuses on the synthesis and assessment of the therapeutic impact of cerium oxide nanoparticles (CeO2 NPs) in rats that have been exposed to aluminum. The effect of CeO2 nanoparticles on the functionality of enzymes and markers related to oxidative stress was assessed in the cerebral and hepatic tissues of rats subjected to aluminum exposure. The enzymes and markers assessed included catalase (CAT), cholinesterase (ChE), malondialdehyde (MDA), total antioxidant capacity (TAC), monoamine oxidase (MAO), reduced glutathione (GSH), and superoxide dismutase (SOD). Aluminum chloride was administered to the rats via subcutaneous injection at a daily dosage of 150 milligrams per kilogram for a duration of three weeks in order to generate oxidative stress. CeO2 nanoparticles (NPs) were administered intraperitoneally at dosages of 5 and 10 mg/kg for a period of one week, with the initial administration occurring in the third week. The findings demonstrated that CeO2 nanoparticles (NPs) were very successful in enhancing cognitive-behavioral patterns and increasing the activity of neurobiochemical enzymes in both liver and brain tissues. The findings indicated that CeO2 NPs might serve as a viable therapeutic approach for addressing neurocognitive and neurobiochemical impairments caused by elevated aluminum levels in rats exposed to aluminum. However, further investigation is necessary to evaluate the therapeutic effectiveness of CeO2 NPs on conditions caused by hazardous metal exposure.

Keywords: CeO2 NPs, Aluminum toxicity, Oxidative Stress, Neurobiochemical Enzymes.

1. Introduction

Neurological and behavioral diseases resulting from exposure to toxic metals, particularly aluminum, persist as a considerable health concern for humans. Aluminum, the most prevalent metal found in the upper mantle, may be introduced into the human body by various means, including dietary intake, oxygen inhalation, water consumption, use of cosmetic products, and some pharmaceuticals (1, 2). Aluminum exposure has been demonstrated to have the potential to induce neurological diseases, given its capacity to affect diverse bodily tissues, with a particular emphasis on the brain. The chemical characteristics of this substance have been demonstrated to inhibit biological functioning and to have deleterious consequences. The absorption and subsequent accumulation of aluminum in the brain may result in the deposition of Aβ oligomers in the hippocampus and cerebral cortex. This process has been observed to be associated with the onset of Alzheimer's disease (3-5). Aluminum has been found to accumulate in tissues other than the brain, including the bone, liver, and kidney. Aluminum pollution in cells has been demonstrated to trigger a disruption of mitochondrial function, resulting in changes to energy metabolism, oxidative stress, and apoptosis. Aluminum has been demonstrated to interfere with neurotransmitter metabolism and signal transmission, which has been linked to neurological complications following exposure (6, 7). The potential consequences of aluminum neurotoxicity may be attributable to a variety of underlying mechanisms. One such mechanism is the potential of aluminum to produce reactive oxygen species (ROS) and free radicals. Furthermore, aluminum has been demonstrated to impede the activity of antioxidant enzymes and disrupt the calcium balance within the body (8). Aluminum, despite its status as a trivalent cation and its inability to undergo redox shifts, has been observed to exacerbate oxidative damage due to its considerable pro-oxidant activity (9). Cells utilize a variety of defense mechanisms to counteract the detrimental effects of reactive oxygen species (ROS). Enzymatic systems, including catalase (CAT), superoxide dismutase (SOD), and glutathione reductase (GR), play a crucial role in safeguarding cellular integrity. Superoxide, a molecule with a negative charge, undergoes a substantial transformation facilitated by the SOD enzyme, resulting in the production of oxygen and hydrogen peroxide. Conversely, catalase plays a pivotal role in decomposing hydrogen peroxide into water and oxygen (10). The proper functioning of the glutathione redox cycle is heavily dependent on the activity of glutathione reductase and helps regulate the concentration of intracellular thiols, namely glutathione, which is the most prevalent (11). Aluminum, a prevalent and readily assimilated metal, has the potential to induce neurological and psychiatric problems. The predominant focus of biomedical research has been on the development of diagnostic and therapeutic techniques using medical nanotechnology for the management of neurological disorders. The focus of this study is ceria, also known as CeO2 nanoparticles, due to their distinctive properties, which have attracted interest. Cerium oxide nanoparticles, also known as ceria, exhibit a lattice fluorite crystalline structure and have been observed to mimic the functions of catalase (CAT) and superoxide dismutase (SOD) enzymes. The catalytic activity of CeO2 nanoparticles exceeds that of SOD and CAT enzymes due to their minute size and elevated surface-to-volume ratio. Therefore, it is imperative to promote the development of effective treatment and diagnostic methods for neurological illnesses (12). The present study assesses the neuroprotective efficacy of CeO2 nanoparticles (NPs) in enhancing cognitive-behavioral patterns and neurobiochemical enzyme activity in rats subjected to aluminum exposure. These nanoparticles demonstrate promise in the management of ailments associated with oxidative stress and inflammation, particularly neurological disorders. The present investigation constitutes the inaugural examination of the neuroprotective properties of CeO2 NPs in rats that have undergone aluminum exposure.

2. Materials and Methods

2.1. CeO2 Nanoparticles Synthesis

A plethora of methodologies are at one's disposal for the synthesis of CeO2 nanoparticles. The synthesis of CeO2 NPs was accomplished through the utilization of the methodical approach delineated by Chelliah et al. (13). The primary precursors employed in this process for the manufacture of cerium oxide are cerium nitrate and sodium hydroxide. The initial step in the experimental procedure involved the preparation of a solution of cerium nitrate with a concentration of 0.1 M. Concurrently, a solution of NaOH with a concentration of 0.3 M was prepared. The NaOH solution was then added to the precursor solution in a gradual manner, while employing a magnetic stirrer to ensure continuous agitation. Consequently, sediment exhibiting a pinkish-white hue was obtained. The sediment was subjected to a centrifugal process at a velocity of 15,000 revolutions per minute for a duration of 15 minutes. The aqueous portion above the sediment, designated as the "supernat," was removed, leaving the solid mass that remained, referred to as the "pellet." The pellet was subsequently subjected to a washing process that involved the use of deionized water and ethanol. Following this step, the material was dried using an oven set at a temperature of 80°C for a duration of one hour. Subsequently, the material was subjected to a process of thermal treatment at a temperature of 270°C, also referred to as "annealing."

2.2. CeO2 Nanoparticles Characterization

A comprehensive examination of the physicochemical properties of the synthesized CeO2 nanoparticles was conducted through the application of diverse analytical techniques. The techniques employed in this study encompassed the use of the Field Emission Scanning Electron Microscope (FE-SEM), thermogravimetric analysis (TGA), Fourier transform infrared (FTIR)

spectroscopy, and X-ray diffraction analysis (XRD). The size and shape characteristics of the generated CeO2 nanoparticles were ascertained through the employment of the FE-SEM technique, utilizing the MIRA3 TESCAN electron microscope. X-ray diffraction (XRD) analysis was employed to ascertain the crystalline structure of the synthesized cerium oxide (CeO_2) nanoparticles. In particular, the Bruker AXS model D8 Advance Diffractometer was utilized for this test. The XRD patterns of the CeO_2 nanoparticles (NPs) were acquired by means of a Cu Ka radiation (k = 1.542 A) X-ray diffractometer. The measurements were conducted within an angular range of 20 to 80°. Fourier transform infrared spectroscopy (FTIR) was utilized to ascertain the chemical composition of the cerium oxide (CeO_2) nanoparticles that were produced. The analysis was conducted using the Bruker Tensor 27 instrument, which is manufactured by Biotage in Germany. The NPs that were produced underwent a process of pulverization, after which they were subsequently mixed with 200 milligrams of potassium bromide (KBr). The resultant powder was then compressed to create standard clear pellets for analysis. Across the frequency spectrum ranging from 400 to 4000 cm-1, a series of 16 scans were conducted to obtain the spectra of the resulting pellets. The Thermogravimetric Analyzer (Linseis STA PT 1000, Germany) was employed to evaluate the thermal stability of CeO2 NPs. The TGA measurements were conducted in a nitrogen environment, spanning a temperature range from room temperature (RT) to 700°C.

2.3. Animals

In this study, male Wistar rats with a body weight ranging from 200 to 250 grams were utilized. The animals were procured from the Pasteur Institute of Iran. The rats were housed in sets of three within a standard cage, ensuring a temperature-controlled environment maintained at 22 ± 2 °C with a 12-hour light and dark cycle. Rats were provided with unrestricted access to water and were fed a conventional diet. The rats were divided into two primary groups: the stress groups and the control groups. The control group, which served as a comparison, did not undergo any form of intervention and had unrestricted access to food and water. Conversely, the stress group received subcutaneous injections of aluminum chloride, with a dosage of 150 milligrams per kilogram of body weight, on a daily basis for a period of three weeks. Subsequently, the stress group was separated into three subgroups two weeks after receiving aluminum: subgroup 1 (AL), subgroup 2 (AL + CeO2 NPs at a dose of 5 mg/kg), and subgroup 3 (AL + CeO2 NPs at a dose of 10 mg/kg). In the third week of the study, CeO2 nanoparticles were administered intraperitoneally for a period of one week.

2.4. Behavioral Assessment

The cognitive functions of rats exposed to aluminum and subsequently treated with CeO2 NPs were evaluated using a shuttle box, measuring both their short-term and long-term memory. The shuttle box is divided into two chambers: a dimly lit room and a brightly illuminated chamber. These chambers are separated by a guillotine door, which allows for the separation of the two spaces. The shuttle box-based behavioral evaluation model is comprised of three phases: adaptation, learning acquisition, and recall. To facilitate acclimation, the animal was exposed to the light chamber for a duration of 10 seconds during the adaptation phase. Subsequent to this, the guillotine door was unlocked, enabling the animal to transition to the dark room, where it remained for approximately 30 seconds. Subsequent to a span of 30 minutes, the aforementioned action was reiterated. The animal was once again exposed to the light chamber during the subsequent learning period, which commenced 30 minutes after the initial phase. Subsequent to the transfer of the animal into the enclosed space devoid of light, the guillotine door was promptly sealed shut, and an electrical shock of 30 seconds duration was administered. After being exposed to an electric shock for 30 seconds, the animal was subsequently confined to a dark location for an additional 30 seconds. Following this, the animal was removed and referred to as having short-term memory. In the third phase, designated as long-term memory, the animal was transferred to the well-lit section after a 24-hour period. This was followed by the subsequent opening of the guillotine door. During this phase, no electric current shock was administered. The investigation focused on three factors: the frequency of transitioning is influenced by the movement from the light chamber to the dark chamber, the duration of time spent in the dark chamber, and the delay in entering the dark chamber from the light chamber. Furthermore, it is imperative to note that the long-term memory stage generally persists for approximately 10 minutes.

2.5. Histopathological Analysis

Following the therapeutic intervention, the animals were euthanized, and their tissues (brain and liver) were extracted for histological investigation. Subsequently, a 10% formalin solution was utilized for the preservation of the tissue samples.

2.6. Determination of Aluminum Content

The aluminum concentration present within the tissues (brain and liver) was measured using the ELAN 6100 DRC-e instrument from Perkin Elmer, employing Inductively Coupled Plasma-Mass Spectrometry (ICP-MS) analysis. To ascertain the aluminum content, 0.5 g of tissue samples (brain or liver) were thoroughly dissolved in 10 ml of nitric acid, employing the application of heat. Subsequently, the solution obtained was subjected to purification via filter paper, followed by dilution to a volume of 50 cc using distilled water. This purified solution was subsequently utilized.

2.7. Biochemical Tests

2.7.1. CAT Activity Determination

Catalase, a pivotal antioxidant enzyme, plays a vital role in the transformation of two hydrogen peroxide molecules into one oxygen molecule and two water molecules.

Catalase dysfunction has been associated with a variety of neurological conditions, including Alzheimer's disease. The decomposition of hydrogen peroxide and the regulation of cellular redox are crucial processes that underscore the significance of catalase (14). The present study evaluated the catalase activity in animal tissues (i.e., the brain and the liver) that were exposed to aluminum and treated with CeO2 NPs. For the present assessment, the NactazTM Catalase Activity Assay Kit (IRAN) was utilized. The methodology is predicated on the response of the CAT enzyme detected in tissue samples. The process under investigation involves the production of formaldehyde, a specific aldehyde, by catalase (CAT). The existence of hydrogen peroxide and methanol as a source of hydrogen donation has been demonstrated to be a prerequisite for this process to occur (15). The process is ultimately halted by the addition of potassium hydroxide. Subsequent quantification of the resulting formaldehyde may be performed through the utilization of spectroscopy, specifically within a wavelength range of 540 to 550 nanometers, in conjunction with a chromogen. Initially, a 100 mg tissue sample (brain/liver) was obtained, rinsed with cold PBS, and then disintegrated in 1 ml of lysing solution to create the tissue homogenate. Subsequently, the mixture underwent a centrifugation process at a rate of 8,000 revolutions per minute for a duration of 10 minutes. The liquid that accumulated above the sediment, designated as the véhicule, was subsequently employed for biochemical examination. Subsequently, the tissue samples were examined for catalase (CAT) activity according to the instructions provided in the kit methodology.

2.7.2. Determination of MAO Activity

Monoamine oxidases (MAOs), a class of enzymes, facilitate the process of oxidative deamination of monoamines. These enzymes are located within the outer membrane of mitochondria. The dysfunction of MAOs, which regulate neurotransmitters, has been linked to various pathologies, including schizophrenia, drug misuse, migraines, depression, and Parkinson's disease (16). A 100 mg sample of tissues (brain or liver) was thoroughly mixed with lysis solution (1 ml) to assess the extent of MAO activity. Subsequent to the application of centrifugal force for a period of 10 minutes at a rate of 8,000 revolutions per minute (RPM), the liquid fraction situated above the sediment was examined via spectrophotometry at a wavelength of 250 nanometers (nm).

2.7.3. Cholinesterase (ChE) Activity Evaluation

Cholinesterase (ChE) is a class of enzymes that catalyzes the hydrolysis of choline esters. This class includes acetylcholinesterase (AChE) and butyrylcholinesterase (BChE). The enzymes in question have been demonstrated to regulate the transmission of nerve signals by rapidly hydrolyzing the neurotransmitter acetylcholine (ACh). This process has been observed to be a potential contributing factor to the development of various neurological disorders, including Alzheimer's disease, depression, and Parkinson's disease (17, 18). In this investigation, the activity of the salt soluble (SS) and detergent soluble (DS) isoforms of AChE and BuChE in animal's tissues (brain and liver) exposed to aluminum and treated with CeO2 NPs was evaluated using Ellman's test and established spectrophotometric techniques. The substrates employed to assess the levels of total cholinesterase (ChE) activity and butyrylcholinesterase (BuChE) activity were acetylthiocholine iodide (ATCh) and S-butyrylthiocholine iodide (BuTCh), respectively. These substrates were obtained from Sigma-Aldrich in the UK and Switzerland, respectively. The measurement of acetylcholinesterase (AChE) activity was determined by the subtraction of butyrylcholinesterase (BuChE) activity from the total cholinesterase (ChE) activity, as demonstrated in references 19 through 22.

2.7.4. Determination of Lipid Peroxidation Level

The production of malondialdehyde (MDA) is a consequential outcome of the peroxidation process that occurs within cells, specifically as a result of unsaturated fatty acids. This compound plays a crucial role as a reliable indicator for evaluating the level of oxidative stress present in the cells. It has been demonstrated that individuals suffering from brain trauma frequently exhibit elevated levels of MDA (23, 24). The NalondiTM lipid peroxidation test kit was utilized to assess the levels of malondialdehyde (MDA) in brain and liver tissue samples. Colorimetry is the method of measuring the extent of the chromogenic compound formation resulting from the interaction between MDA and thiobarbituric acid (TBA). This fundamental principle establishes the basis for the technique. In summary, a 100-mg tissue sample (either brain or liver) was combined with 1 ml of lysing buffer. Subsequently, the resulting blend underwent a centrifugation process at a velocity of 13,000 RPM for a duration of three minutes. The analysis of the aqueous component was then conducted using a spectrophotometer set at a wavelength of 550 nm, in accordance with the guidelines outlined in the kit, to determine the concentration of malondialdehyde (MDA).

2.7.5. Determining Reduced Glutathione (GSH) Level

Within the human body, Glutathione (GSH) plays an indispensable role as a cellular constituent, accounting for 95% of non-protein thiol groups. The levels of GSH present in various organs exhibit fluctuations, and imbalances in GSH levels and enzyme activity have the potential to contribute to the onset of neurodegenerative diseases. GSH fulfills a variety of functions within cells, including its role as a redox buffer, a cofactor for signal transduction, and an antioxidant defense mechanism. Its significance is particularly notable in the brain, where it plays a crucial role in maintaining cellular homeostasis and protecting against oxidative stress (25, 26). The level of GSH in the brain and liver tissues of animals exposed to aluminum and treated with CeO2 NPs was measured using the NarGulTM test kit for reduced glutathione (GSH). Initially, a 100 mg tissue sample was thoroughly mixed with lysing buffer, followed by centrifugation at a speed of 9,000 revolutions per minute for a duration of 15 minutes. The established methodology

was employed to assess the optical absorbance of the tissue sample through spectrophotometry at a wavelength of 412 nanometers (nm).

2.7.6. Determination of SOD Activity

The decomposition of superoxide into oxygen and hydrogen peroxide is a foundational process that transpires within cells, and it is facilitated by the indispensable enzyme known as superoxide dismutase (SOD). The primary objective of this study is to regulate reactive oxygen and nitrogen species (ROS and NOS), thereby mitigating their potential adverse effects and preventing diseases associated with oxidative stress in cells and extracellular environments (27, 28). The assay kit for measuring the activity of superoxide dismutase (SOD) was used to evaluate the amount of SOD activity in brain and liver tissue samples. The tissue sample was initially combined with lysing buffer at a concentration of 100 mg. Subsequently, the mixture was homogenized and subjected to centrifugation at a speed of 12,000 RPM for a period of 5 minutes. The quantification of superoxide dismutase (SOD) activity was performed using a spectrophotometric technique at a wavelength of 405 nm. The kit's protocol was followed to ensure the accurate measurement of the samples.

2.7.7. Total Antioxidant Capacity (TAC) Evaluation

The concept of total antioxidant capacity (TAC) encompasses the collective effect exerted by the entirety of antioxidants existing within a given matrix, be it bodily fluids or dietary elements. The evaluation of TAC levels in liver and brain tissue samples was conducted through the utilization of a total antioxidant capacity test kit. This kit utilizes the FRAP approach, a process involving the transfer of a single electron, to assess the potential of biomolecules to undergo bivalent reduction and their capability to act as antioxidants. The tissue homogenate was prepared by adding a lysing buffer to 100 milligrams of tissue samples. The mixture was subsequently subjected to homogenization and centrifugation at a speed of 10,000 RPM for a duration of 10 minutes. The total antioxidant capacity (TAC) was subsequently determined by operating a spectrophotometer at 593 nm wavelength, following the instructions outlined in the provided kit.

2.8. Statistical Analysis

The statistical analysis was performed using SPSS 27 and GraphPad Prism 9 software packages. The statistical significance of the comparisons was assessed through the application of the one-way analysis of variance (ANOVA) method. The statistical significance was determined by employing a significance level of $P<0.05$. The data were presented in the form of mean ± standard deviation (SD).

3. Results

3.1. Characterization of CeO2 NPs

3.1.1. FE-SEM Analysis of CeO2 NPs

The FE-SEM technique was employed to examine the morphology and surface characteristics of CeO2 nanoparticles. Figure 1.a demonstrates that CeO2 NPs had a spherical shape and were of nanoscale dimensions, In accordance with the discoveries made by Chelliah et al., the results remain in line with their research (13). The CeO2 nanoparticles produced in this work had an average size ranging from 36.84 to 73.68 nm.

3.1.2. FTIR Analysis

The chemical composition of the produced nanoparticles was subsequently analyzed using FT-IR analysis. The significant peak observed at 3499 cm-1 in the infrared (IR) spectra of CeO2 NPs is attributed to the stretching vibrations of hydroxyl groups. The maximum absorption peak observed at 1559 cm-1 is attributed to the bending vibration of the C-H stretching mode. Furthermore, the band observed at the location of 1058 cm-1 indicates the C-O stretching vibration. The synthesis of CeO_2 nanoparticles was confirmed through the analysis of the FTIR spectrum (Figure 1b).

3.1.3. XRD Analysis

As illustrated in Figure 1c, the XRD analysis reveals the unique peaks of cerium oxide nanoparticles (CeO_2 NPs) at 28.64, 33.16, 47.56, and 56.38 degrees. As indicated in Reference 13, these peaks correspond to the JCPDS No. 34-0394 reference pattern.

3.1.4. Thermal Analysis

The thermal stability of the produced nanoparticles was assessed using the Thermogravimetric Analysis (TGA) method in a nitrogen environment. Figure 1d illustrates the pyrolysis curve employed for the analysis of the thermal properties of the produced CeO2 nanoparticles. The pyrolysis curve of CeO_2 NPs demonstrated a weight reduction of approximately 1% within the temperature range of 30 to 100°C, and a weight reduction of roughly 3% within the temperature range of 100 to 700°C.

3.2. Accumulation of Aluminum in Animal Tissues (lLiver and Brain)

The ICP-MS technique was employed to measure the levels of aluminum in animal tissues (brain and liver) exposed to aluminum, as presented in Table 1. As illustrated in Table 1, the results of the ICP-MS analysis revealed a substantial accumulation of aluminum in the brain tissues, particularly in the liver tissues, of the treated animals. The findings indicate that the injection of CeO2 NPs may effectively clean and minimize the buildup of aluminum in both liver and brain tissues.

3.3. Serum Biochemical Parameters

3.3.1. CAT Activity

As illustrated in Figure 2, the study examined the effects of aluminum exposure and CeO2 NPs administration on catalase enzyme activity in rat tissues, specifically the brain and liver. As illustrated in Figure 2, a substantial decrease in catalase enzyme activity was observed in the tissues of rats (brain and liver) following aluminum administration. The administration of CeO2 NPs resulted in an increase in catalase enzyme activity in the liver and brain tissues, as had been predicted. A notable finding was that the administration of a dosage of 10 mg/kg resulted in a more significant elevation in catalase activity levels in both brain

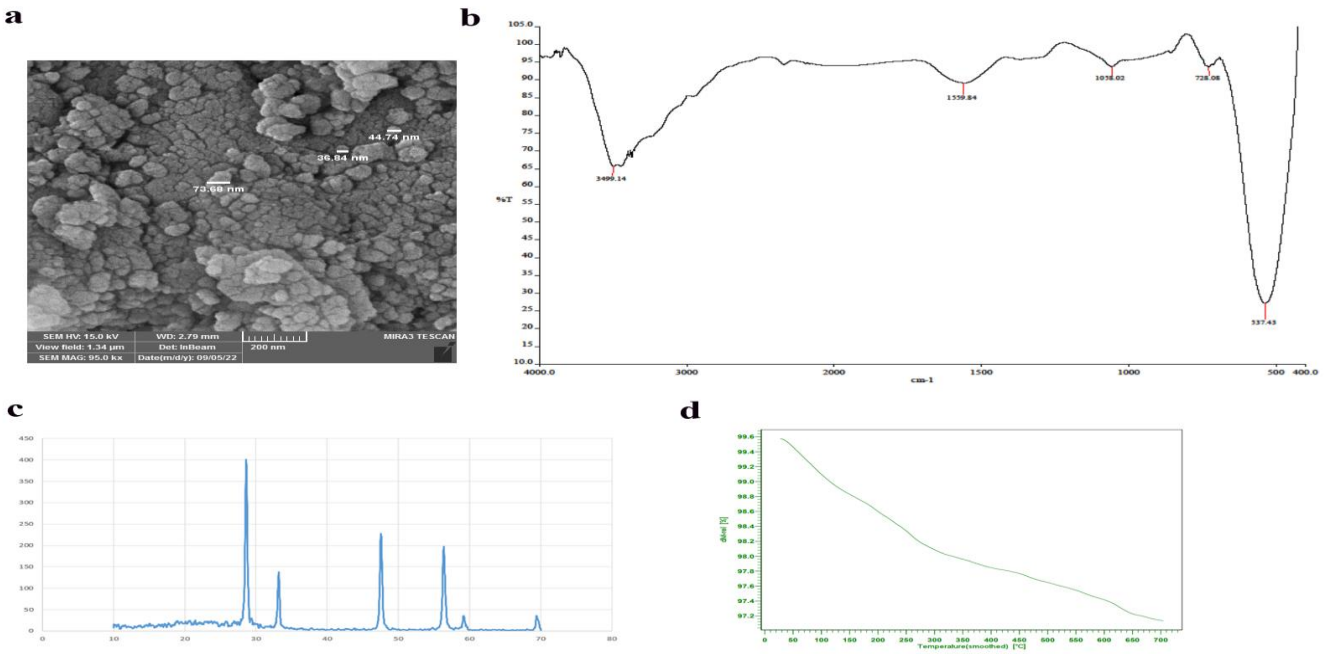

Figure 1. Nanoparticles Characterization. a) FE-SEM image, b) FTIR spectrum, c) XRD patterns, and d) Thermal analysis of synthesized CeO2 NPs.

Table 1. The amount of aluminum accumulation in brain and liver tissues.

Mice groups	Brain	Liver
Control	0.28 ±0.2	2.91 ±0.6
Al treated	2.16 ±0.3 ***	9.19 ±0.2 ***
Al+ CeO_2 5 mg/kg	0.41 ±0.5**	5.64 ±0.3 ***
Al+ CeO_2 10 mg/kg	0.11 ±0.1 ***	4.15 ±0.5 ***

The data represent the mean ± SEM, statistically significant differences from the control group (**P < 0.01, ***P < 0.001, Tukey's test).

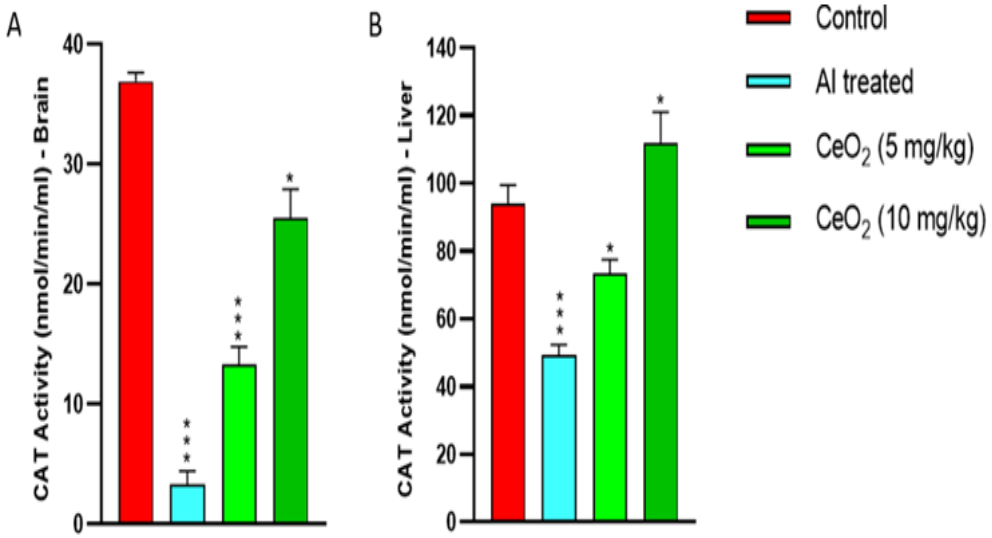

Figure 2. The graphs illustrate the CAT activity in the brain (A) and liver (B) tissues of rats exposed to aluminum and received CeO2 NPs.

and liver tissues than the administration of a 5 mg/kg dosage.

3.3.2. MDA Levels

As illustrated in Figure 3, the concentrations of MDA (malondialdehyde) in rat tissues (brain and liver) that received aluminum and then were treated with CeO2 NPs (cerium oxide nanoparticles) are shown. As illustrated in Figure 1, the injection of aluminum resulted in a modest increase in the concentration of MDA in the tissues of rats (brain and liver). The present study has demonstrated that the administration of CeO2 nanoparticles has resulted in a reduction in MDA activity when compared to the aluminum-exposed group and the control group. Nevertheless, CeO2 nanoparticles have not demonstrated any significant impact on liver tissue.

3.3.3. GSH Contents

As illustrated in Figure 4, the levels of glutathione (GSH) in the tissues of rats (brain and liver) have been examined following the administration of aluminium and subsequent treatment with cerium oxide nanoparticles (CeO2 NPs). As demonstrated in Figure 4, there was a significant decrease in brain tissue GSH levels in animals that received aluminium. However, the presence of aluminium did not have a discernible impact on the concentration of GSH in the liver tissue. The administration of CeO2 NPs at a concentration of 10 mg/kg resulted in an increase in the concentration of GSH within the brain tissue. The present study demonstrated a significant increase in the concentration of GSH in the liver tissue of the experimental group in comparison to the control group, following the administration of CeO2 NPs.

3.3.4. TAC Levels

As illustrated in Figure 5, the concentrations of TAC (total antioxidant capacity) in the tissues of rats (brain and liver) that received aluminium and were subsequently treated with CeO2 NPs (cerium oxide nanoparticles) are displayed. The Figure indicates that the injection of aluminium did not result in a substantial alteration in the levels of TAC within brain tissue. However, the introduction of aluminium infusion has been demonstrated to result in a significant decrease in TAC levels in liver tissue. The administration of CeO_2 NPs, at both dosages, has been demonstrated to result in a substantial augmentation of the total antioxidant capacity (TAC) within the hepatic tissue.

3.3.5. SOD Activity

As illustrated in Figure 6, the level of superoxide dismutase (SOD) activity in the brain and liver tissues of rats is shown. These rats had been exposed to aluminum and subsequently treated with cerium oxide nanoparticles (CeO_2 NPs). Rats that had been administered aluminum exhibited a significant decrease in SOD activity in their liver tissue; however, only a minor decline was observed in their brain tissue. The administration of CeO2 nanoparticles has been demonstrated to result in elevated superoxide dismutase (SOD) activity in the tissues of rats (brain and liver).

3.3.6. MAO Activity

As illustrated in Figure 7, the degree of activity of the MAO enzyme in the brain tissue of rats that received aluminum and CeO2 NPs is depicted. As demonstrated in Figure 1, the incorporation of aluminum and CeO2 nanoparticles did not result in a discernible change in the level of MAO activity.

3.4. Memory and Behavioral Patterns

The present study evaluated the behavioral patterns and memory of rats that had been exposed to aluminum and administered CeO2 nanoparticles. The animals were confined within a dimly illuminated enclosure, subjected to a gradual transition from a well-lit area to a dark room, and then transferred from the illuminated area to the dark chamber. In the aftermath of the electric shock, the control group demonstrated an inability to remain in the dark room. The exposure to aluminium resulted in an extended period of time spent in the dark room. The administration of CeO2 nanoparticles resulted in increased animal activity and decreased persistence rates in the dark region. Rats that received aluminium exhibited a reduced latency in moving from the illuminated room to the dark room, when compared to the control group. Nevertheless, the administration of CeO2 nanoparticles enhanced behavioral patterns and decreased the frequency of entering the dark room. The control group demonstrated no movement from the brightly illuminated chamber to the dimly illuminated space. However, aluminium exposure resulted in cognitive impairment and disorientation (Figure 8).

3.5. Cholinesterase Activity

The research demonstrates that exposure to aluminium in rats results in a marked decrease in the activity of both the SS and DS isoforms of AChE in brain tissue, in comparison to the control group. Nevertheless, the introduction of CeO2 nanoparticles (NPs) mitigated the impact of aluminium on these isoforms, resulting in an augmentation of their activity in brain tissue. Furthermore, a decline in all isoforms of AChE (SS and DS) was observed in the liver tissue of rats that received aluminium. Nevertheless, the introduction of CeO2 nanoparticles enhanced the performance of these isoforms in liver tissue. Conversely, the presence of aluminium led to a decrease in the activity of the SS isoform of BuChE in brain tissue, while the DS isoform exhibited a modest increase. The activity of the SS isoform in the brain exhibited a significant decline following the administration of CeO2 nanoparticles at a dosage of 5 mg/kg. Furthermore, an enhancement was observed with the 10 mg/kg dosage. The hepatic tissue of rats exposed to aluminium exhibited a decrease in the activity of all isoforms of BuChE (SS and DS) (Table 2).

3.6. Histopathological Parameters

As illustrated in Figures 9 and 10, the histopathological appearances of rat brain and liver tissues that were exposed to aluminium and administered CeO2 nanoparticles are evident. The examination of histological pictures revealed aberrant alterations in the morphology of neurons, as well as the initiation of programmed cell death, known as

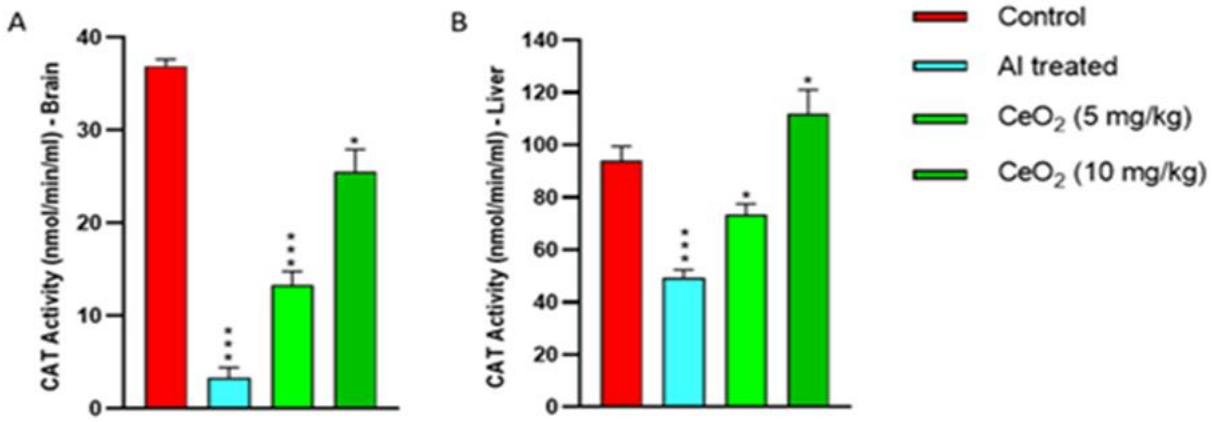

Figure 3. MDA level in the brain (A) and liver (B) tissues of rats exposed to aluminum and received CeO2 NPs.

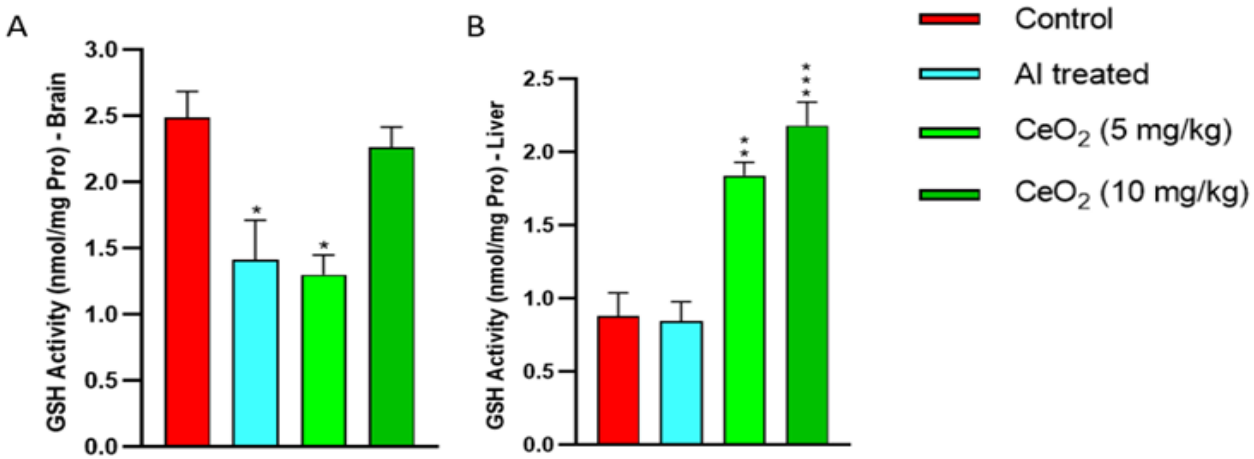

Figure 4. GSH level in brain (A) and liver (B) tissues of rats exposed to aluminum and received CeO2 NPs.

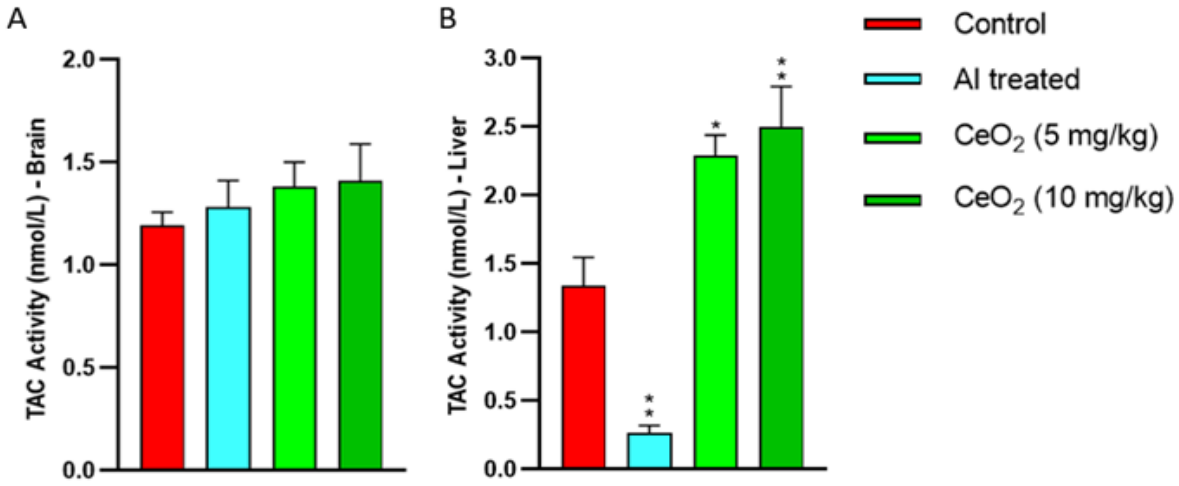

Figure 5. TAC level in brain (A) and liver (B) tissues of rats exposed to aluminum and received CeO2 NPs.

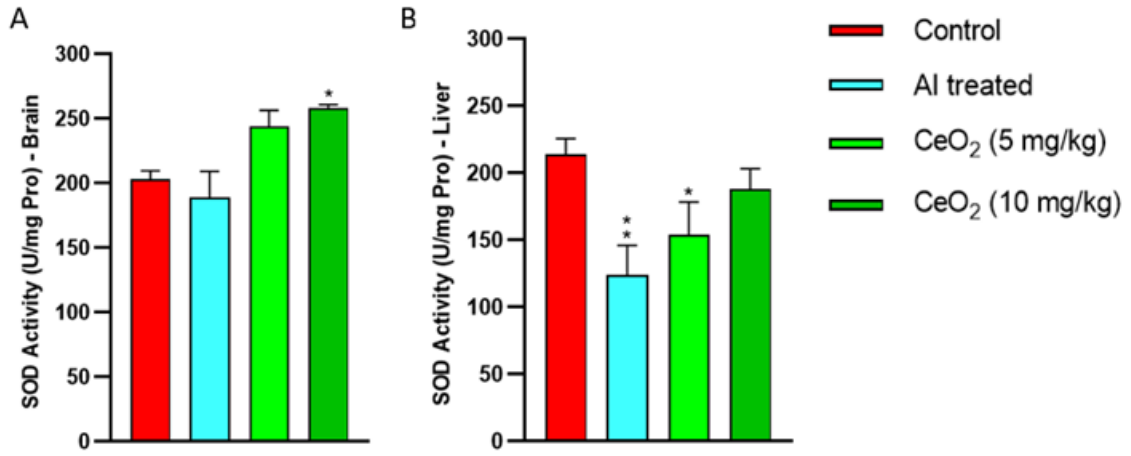

Figure 6. SOD activity in the brain (A) and liver (B) tissues of rats exposed to aluminum and received CeO2 NPs.

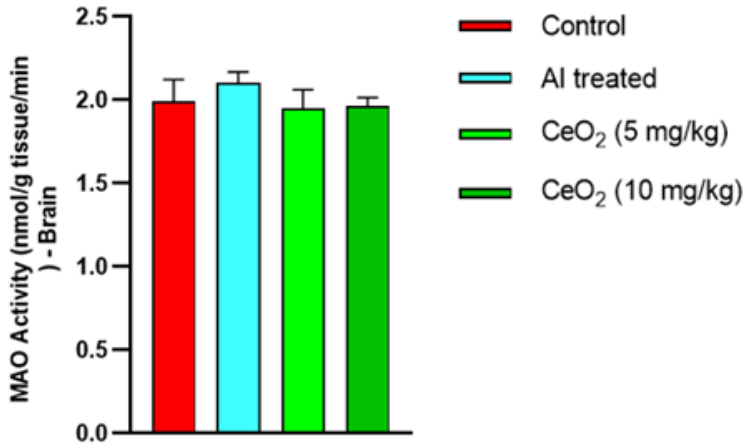

Figure 7. MAO activity in brain tissue of rats exposed to aluminum and received CeO2 NPs.

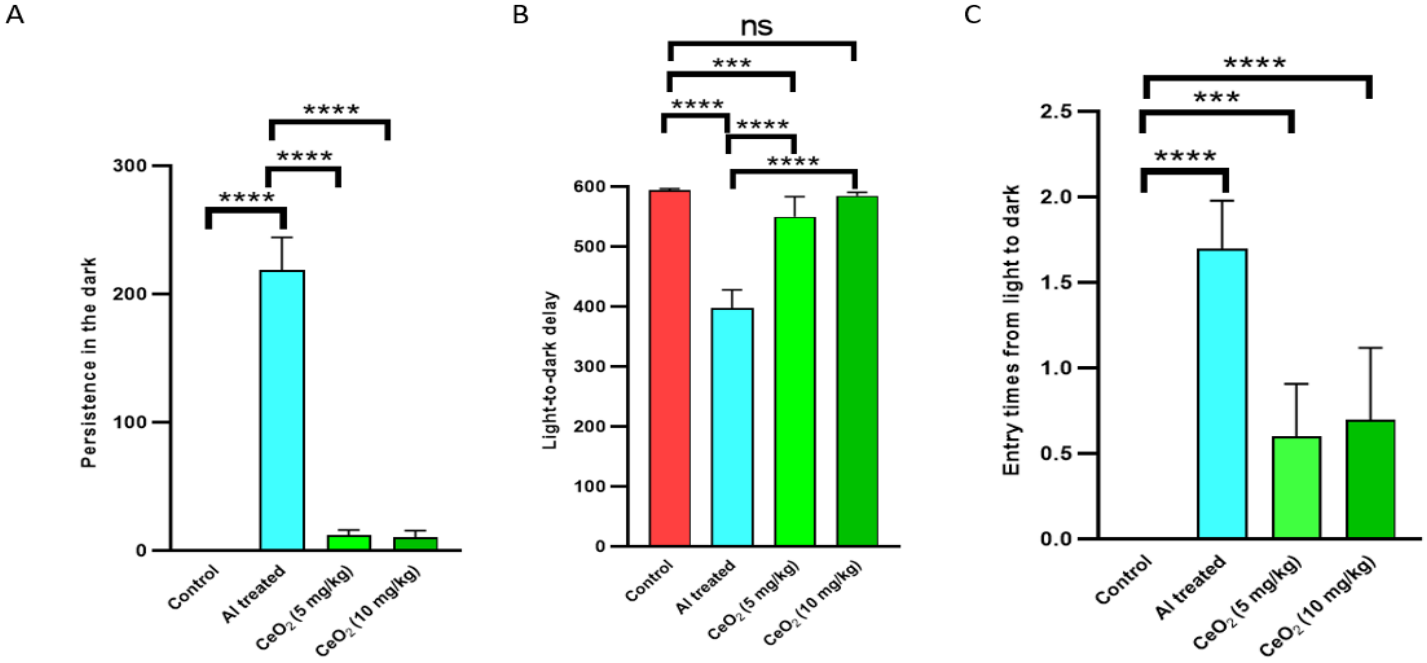

Figure 8. The graphs illustrate of memory and behavioral patterns of animals exposed to aluminum or received cerium oxide NPs. A) Persistence in the dark chamber, B) Light-to-dark delay and C) Entry times from light to dark.

Table 2. The purpose of this study is to examine the functionality of AChE and BuChE isoforms, specifically SS and DS, in rat tissues, namely the brain and the liver.

Enzymes	Groups	Whole Brain (-ce)		Liver	
		SS-ChE	DS-ChE	SS-ChE	DS-ChE
AChE activity (µmol/min/g tissue)	Control	13.27	81.94	3.43	0.81
	Al treated	8.22***	58.72***	2.48	0.52*
	Al + CeO2 5 mg/kg	9.46***	62.13*	2.65	0.53
	Al + CeO2 10 mg/kg	11.25**	73.28	2.98	0.66
BuChE activity (µmol/min/g tissue)	Control	1.89	2.28	25.86	8.80
	Al treated	1.59	2.34	19.64***	5.70*
	Al + CeO2 5 mg/kg	1.65	2.38	20.35**	6.08
	Al + CeO2 10 mg/kg	1.74	2.24	23.43	7.19

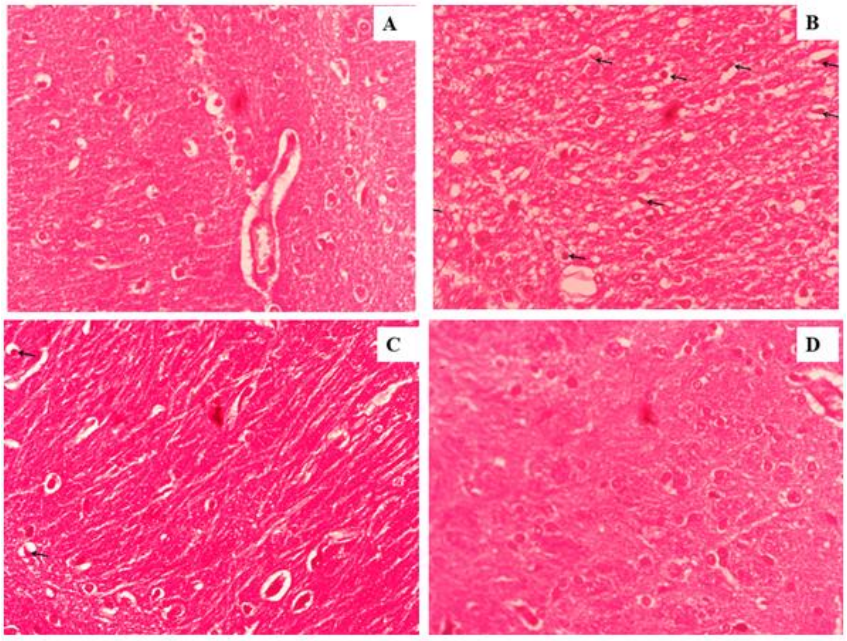

Figure 9. Photomicrographs of hippocampus tissue following hematoxylin and eosin staining. Control group (A), Al treated group showing increased apoptotic neurons with dystrophic changes in the form (arrows) (B), CeO2 NPs 5 mg/kg (C) and CeO2 NPs 10 mg/kg, magnification 400× (D).

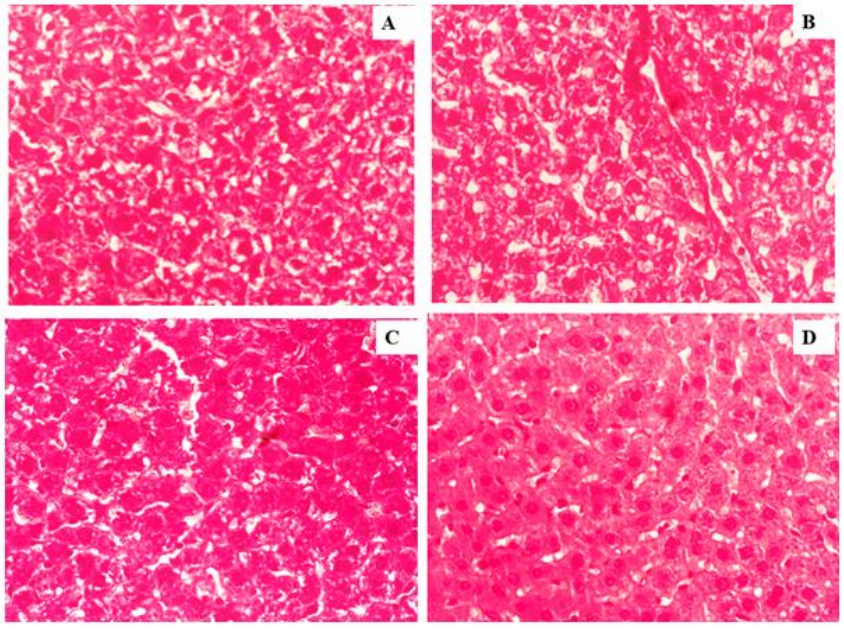

Figure 10. Photomicrographs of liver tissue following hematoxylin and eosin staining showed no alteration in any groups. Control group (A), Al treated group (B), CeO2 NPs 5 mg/kg (C) and CeO2 NPs 10 mg/kg, magnification 400× (D).

apoptosis, in mice that were subjected to aluminium exposure.

4. Discussion

Elevated exposure to aluminium has been demonstrated to be a contributing factor to the onset of neurodegenerative diseases, including dementia and Alzheimer's disease. In summary, the accumulation of aluminium in the human body can lead to the deterioration of neurofibrils. Aluminium poisoning primarily affects the brain, where it accumulates and causes impairments in regions associated with memory and learning (7, 29, 30). CeO2 nanoparticles, which are extensively utilised and highly efficient, possess strong antioxidative characteristics and have the potential to inhibit free radicals. In their study, Ranjbar et al. sought to evaluate the impact of CeO2NPs on oxidative toxic stress damage in the brain caused by PQ. The results of the study demonstrated that CeO2 NPs exhibited neuroprotective and antioxidant properties in brain damage caused by PQ (31). In a study of stress-induced models of depression, Zavvari et al. demonstrated the neuroprotective and neural plasticity effects of CeO2NPs. Elevated exposure to aluminium has been demonstrated to be a contributing factor to the onset of neurodegenerative diseases, including dementia and Alzheimer's disease. In summary, the accumulation of aluminium in the human body can lead to the deterioration of neurofibrils. Aluminium poisoning primarily affects the brain, where it accumulates and causes impairments in regions associated with memory and learning (7, 29, 30). CeO2 nanoparticles, which are extensively utilised and highly efficient, possess strong antioxidative characteristics and have the potential to inhibit free radicals. In their study, Ranjbar et al. sought to evaluate the impact of CeO2NPs on oxidative toxic stress damage in the brain caused by PQ. The results of the study demonstrated that CeO2 NPs exhibited neuroprotective and antioxidant properties in brain damage caused by PQ (31). In a study of stress-induced models of depression, Zavvari et al. demonstrated the neuroprotective and neural plasticity effects of CeO2NPs. Benyettou et al. conducted a study which revealed that exposure to aluminium leads to the occurrence of oxidative stress and behavioral alterations (30). The investigation comprised the intraperitoneal delivery of CeO2NPs to rats, with two different doses. The evaluated biomarkers included CAT, MDA, SOD, GSH, and other enzymes. The study revealed a substantial decline in CAT activity within the rats' tissues (brain and liver) upon exposure to aluminium. However, the administration of CeO2NPs, particularly at elevated doses, has been observed to result in an enhancement in CAT activity, suggesting a beneficial effect of CeO2NPs. Lipid peroxidation is defined as the process of oxidative degradation of fatty acids with numerous double bonds in the cell membrane, resulting in damage. MDA, generated during continuous oxidative breakdown, impacts the function of other molecules and the overall cellular activity. A minor increase in MDA levels was detected in brain tissues subsequent to aluminium infusion. The application of CeO2NPs has been observed to both enhance and decrease the levels of MDA in animal tissues, including the brain and liver. The administration of CeO2NPs at a higher dosage resulted in elevated levels of GSH in brain tissue and a notable rise in GSH levels in liver tissue when compared with the control group. In the present study, aluminium exposure was found to result in diminished superoxide dismutase (SOD) activity in the liver tissue of test subjects in comparison with their brain tissue. However, the presence of cerium oxide nanoparticles (CeO2NPs) boosted SOD activity in both brain and liver tissues. The levels of TAC in animal tissues exhibited a notable reduction in liver tissue, but the administration of aluminum and CeO2 NPs did not induce substantial alterations in MAO activity levels. The levels of AChE and BuChE isoforms (SS and DS) were seen to decrease in animal tissues (brain and liver). However, the presence of CeO2NPs dramatically enhanced the activity of these isomers. Histopathological examinations revealed heightened apoptosis in neurons and dystrophic alterations in tissue morphology, although no notable modifications were seen in liver tissue. Similarly, in other studies, the antioxidant and neuroprotective effects of cerium oxide nanoparticles have been observed, for example: In an attempt by Dutta et al., the pro-oxidant (toxic effect) and antioxidant (protective effect) activity of cerium oxide nanoparticles synthesized in different conditions was evaluated in zebrafish as a model system (34). The results obtained from this study showed that cerium oxide nanoparticles synthesized in alkaline pH do not show any toxic effects. However, cerium oxide nanoparticles synthesized at acidic pH showed significant toxic effect (34). Antioxidant and neuroprotective activity of cerium oxide nanoparticles in mouse ischemia model was shown by Estevez et al (35). In a study by Elshony et al., the ameliorative effects and antioxidant activity of cerium oxide nanoparticles against the effect of fipronil on brain function, apoptotic cascades, and oxidative stress were investigated (36). The results of this study showed that the treatment with cerium oxide nanoparticles led to the transformation of the degenerative changes resulting from the effects of fipronil on the brain tissue to an almost normal brain structure. Generally, the results obtained from this study indicate the antioxidant activity of cerium oxide nanoparticles against the toxic effects of fipronil (36). The results of this study showed that the treatment with cerium oxide nanoparticles led to the transformation of the degenerative changes resulting from the effects of fipronil on the brain tissue to an almost normal brain structure. Generally, the results obtained from this study indicate the antioxidant activity of cerium oxide nanoparticles against the toxic effects of fipronil (36). The findings indicate that rats exposed to aluminium exhibit significant impairments in both behavioural and cognitive functions. Moreover, biochemical analysis has demonstrated that rats exposed to aluminium exhibit a decline or disruption in the levels of CAT, MDA, SOD, GSH, ChE, and TAC. The utilisation of

CeO2NPs in this investigation resulted in a substantial enhancement in behavioural-cognitive patterns and neurobiochemical enzyme activity, thereby signifying the considerable therapeutic effectiveness of CeO2 NPs.

Acknowledgment
It is important to acknowledge the support provided to us by the Department of Biology at the Faculty of Natural Sciences, University of Tabriz, Tabriz, Iran, and the Department of Biology at the Faculty of Science, University of Mohaghegh Ardabili, Ardabil, Iran, during the course of the study.

Authors' Contribution
Study concept and design: A. A, D.G
Acquisition of data: M.D, A. AS, G.A
Analysis and interpretation of data: A.A, D.G,
Drafting of the manuscript: A.A, D.G, G.H
Critical revision of the manuscript for important intellectual content: M.D, A.AS, G.A, A.A, D.G
Statistical analysis: A.A, D.G, G.H
Administrative, technical, and material support: A.A, D.G

Ethics
The experimental methodology was conducted in accordance with the guidelines provided in the "NRC Guide for the Care and Use of Laboratory Animals: 8th ed." Furthermore, the study was conducted in strict accordance with the guidelines and standards stipulated by the Research Ethics Committee, with approval being granted by the Research Ethics Committees of Tabriz University. This is in accordance with the ethical code IR.TABRIZU.REC.1401.044.

Conflict of Interest
The authors declare no conflict of interest in this research.

Funding
This work was supported by the Department of Biology, Faculty of Natural Sciences, University of Tabriz, Tabriz, Iran.

Data Availability
The data that support the findings of this study are available on request from the corresponding author.

References

1. Fernandes RM, Eiró LG, dos Santos Chemelo V, Alvarenga MOP, Lima RR. Aluminum toxicity and oxidative stress. Toxicology: Elsevier; 2021. p. 35-127.
2. Rahimzadeh MR, Rahimzadeh MR, Kazemi S, Amiri RJ, Pirzadeh M, Moghadamnia AA. Aluminum poisoning with emphasis on its mechanism and treatment of intoxication. Emergency medicine international. 2022.
3. Mold MJ, O'Farrell A, Morris B, Exley C. Aluminum and tau in neurofibrillary tangles in familial Alzheimer's disease. Journal of Alzheimer's Disease Reports. 2021;5(1):94-283.
4. Das N, Raymick J, Sarkar S. Role of metals in Alzheimer's disease. Metabolic brain disease. 2021;36(7):39-1627.
5. Liu Y, Nguyen M, Robert A, Meunier B. Metal ions in Alzheimer's disease: a key role or not0 Accounts of chemical research. 2019;52(7); 2026-35.
6. Cheng H, Yang B, Ke T, Li S, Yang X, Aschner M, et al. Mechanisms of metal-induced mitochondrial dysfunction in neurological disorders. Toxics. 2021;9(6):142.
7. Kumar V, Gill KD. Oxidative stress and mitochondrial dysfunction in aluminium neurotoxicity and its amelioration: a review. Neurotoxicology. 2014;(41):154-66.
8. Sadauskiene I, Liekis A, Staneviciene I, Naginiene R, Ivanov L. Effects of long-term supplementation with aluminum or selenium on the activities of antioxidant enzymes in mouse brain and liver. Catalysts. 2020;10(5):585.
9. Campbell A, Prasad KN, Bondy SC. Aluminum-induced oxidative events in cell lines: glioma are more responsive than neuroblastoma. Free Radical Biology and Medicine. ١٩٩٩;٢٦(١٠-٩):.٧١-١١٦٦
10. Chelikani P, Fita I, Loewen PC. Diversity of structures and properties among catalases. Cellular and Molecular Life Sciences CMLS. ٢٠٠٤;.٢٠٨-٦١:١٩٢
11. Couto N, Wood J, Barber J. The role of glutathione reductase and related enzymes on cellular redox homoeostasis network. Free radical biology and medicine. ٢٠١٦;.٤٢-٩٥:٢٧
12. Nelson BC, Johnson ME, Walker ML, Riley KR, Sims CM. Antioxidant cerium oxide nanoparticles in biology and medicine. Antioxidants. ٢٠١٦;٥(٢):.١٥
13. Chelliah M, Rayappan JBB ,Krishnan UM. Synthesis and characterization of cerium oxide nanoparticles by hydroxide mediated approach. Journal of Applied Sciences. ٢٠١٢;١٢(١٦):.٧-١٧٣٤
14. Nandi A, Yan L-J, Jana CK, Das N. Role of catalase in oxidative stress-and age-associated degenerative diseases. Oxidative medicine and cellular longevity. ٢٠١٩;.٢٠١٩
15. Sies H. Role of metabolic H٢O ٢generation: redox signaling and oxidative stress. Journal of Biological Chemistry. ٢٠١٤;٢٨٩(١٣):.٤١-٨٧٣٥
16. Ghosal A. Evaluation of the clearance mechanism of non-CYP-mediated drug metabolism and DDI as a victim drug. Identification and Quantification of Drugs, Metabolites, Drug Metabolizing Enzymes, and Transporters: Elsevier; ٢٠٢٠. p. .٧١-٢٣٧
17. Askar KA, Kudi AC, Moody AJ. Comparative analysis of cholinesterase activities in food animals using modified Ellman and Michel assays. Canadian Journal of Veterinary Research. ٢٠١١;٧٥(٤):.٧٠-٢٦١
18. Ma Y, Gao W, Ma S, Liu Y, Lin W. Observation of the elevation of cholinesterase activity in brain glioma by a near-infrared emission chemsensor. Analytical Chemistry. ٢٠٢٠;٩٢(١٩):.١٠-١٣٤٠٥

19. Ellman GL, Courtney KD, Andres Jr V, Featherstone RM. A new and rapid colorimetric determination of acetylcholinesterase activity. Biochemical pharmacology. ١٩٦١;.٩٥-٨٨:(٢)٧
20. Lassiter T, Barone Jr S, Padilla S. Ontogenetic differences in the regional and cellular acetylcholinesterase and butyrylcholinesterase activity in the rat brain. Developmental brain research. ١٩٩٨;١٠٥(١):.٢٣-١٠٩
21. Papandreou MA, Tsachaki M ,Efthimiopoulos S, Cordopatis P, Lamari FN, Margarity M. Memory enhancing effects of saffron in aged mice are correlated with antioxidant protection. Behavioural brain research. ٢٠١١;٢١٩(٢):.٢٠٤-١٩٧
22. Linardaki ZI, Orkoula MG, Kokkosis AG, Lamari FN, Margarity M. Investigation of the neuroprotective action of saffron (Crocus sativus L.) in aluminum-exposed adult mice through behavioral and neurobiochemical assessment. Food and Chemical Toxicology. ٢٠١٣;.٧٠-٥٢:١٦٣
23. Wang X, Zhang D, Song W, Cai CF, Zhou Z, Fu Q, et al. Neuroprotective effects of the aerial parts of Polygala tenuifolia Willd extract on scopolamine‐induced learning and memory impairments in mice. Biomedical Reports. ٢٠٢٠;١٣(٥):.-١
24. Gaweł S, Wardas M, Niedworok E, Wardas P. Malondialdehyde (MDA) as a lipid peroxidation marker. Wiadomosci lekarskie (Warsaw, Poland: ١٩٦٠). ٢٠٠٤;٥٧(١٠-٩):.٥-٤٥٣
25. Aoyama K, Nakaki T. Impaired glutathione synthesis in neurodegeneration. International journal of molecular sciences. ٢٠١٣;١٤(١٠):.٤٤-٢١٠٢١
26. Johnson WM, Wilson-Delfosse AL, Mieyal JJ. Dysregulation of glutathione homeostasis in neurodegenerative diseases. Nutrients. ٢٠١٢;٤(١٠):-١٣٩٩ .٤٤٠
27. Wang Y, Branicky R, Noë A, Hekimi S. Superoxide dismutases: Dual roles in controlling ROS damage and regulating ROS signaling. Journal of Cell Biology. ٢٠١٨;٢١٧(٦):.٢٨-١٩١٥
28. Assady M, Farahnak A, Golestani A, Esharghian M. Superoxide dismutase (SOD) enzyme activity assay in Fasciola spp. parasites and liver tissue extract. Iranian journal of parasitology. ٢٠١١;٦(٤):.١٧
29. Bihaqi SW, Sharma M, Singh AP, Tiwari M. Neuroprotective role of Convolvulus pluricaulis on aluminium induced neurotoxicity in rat brain. Journal of ethnopharmacology. ٢٠٠٩;١٢٤(٣):.١٥-٤٠٩
30. Benyettou I, Kharoubi O, Hallal N, Benyettou HA, Tair K, Belmokhtar M, et al. Aluminium-induced behavioral changes and oxidative stress in developing rat brain and the possible ameliorating role of Omega-٦/Omega- ٣ratio. J Biol Sci. ٢٠١٧;١٧(٣):.١٧-١٠٦
31. Ranjbar A, Soleimani Asl S, Firozian F, Heidary Dartoti H, Seyedabadi S, Taheri Azandariani M, et al. Role of cerium oxide nanoparticles in a paraquat-induced model of oxidative stress: emergence of neuroprotective results in the brain. Journal of Molecular Neuroscience. ٢٠١٨;.٧-٦٦:٤٢٠
32. Zavvari F, Nahavandi A, Shahbazi A. Neuroprotective effects of cerium oxide nanoparticles on experimental stress-induced depression in male rats. Journal of Chemical Neuroanatomy. ٢٠٢٠;.١٠٦:١٠١٧٩٩
33. Soluki M, Mahmoudi F, Abdolmaleki A, Asadi A, Sabahi Namini A. Cerium oxide nanoparticles as a new neuroprotective agent to promote functional recovery in a rat model of sciatic nerve crush injury. British Journal of Neurosurgery. .٦-٢٠٢٠:١
34. Dutta D, Mukherjee R, Ghosh S, Patra M, Mukherjee M, Basu T. Cerium oxide nanoparticles as antioxidant or pro-oxidant agents. ACS Applied Nano Materials. ٢٠٢٢;٥(١):.٧٠١-١٦٩٠
35. Estevez AY, Ganesana M, Trentini JF, Olson JE, Li G, Boateng YO, et al. Antioxidant enzyme-mimetic activity and neuroprotective effects of cerium oxide nanoparticles stabilized with various ratios of citric acid and EDTA. Biomolecules. ٢٠١٩;٩(١٠):.٥٦٢
36. Elshony N, Nassar AM, El-Sayed YS, Samak D, Noreldin A, Wasef L, et al. Ameliorative role of cerium oxide nanoparticles against fipronil impact on brain function, oxidative stress, and apoptotic cascades in albino rats. Frontiers in Neuroscience. ٢٠٢١;.١٥:٦٥١٤٧١